Dynamic association of the PI3P-interacting Mon1-Ccz1 GEF with vacuoles is controlled through its phosphorylation by the type 1 casein kinase Yck3

Gus Lawrence[a,*], Christopher C. Brown[a,*], Blake A. Flood[a,*], Surya Karunakaran[a], Margarita Cabrera[b], Mirjana Nordmann[b], Christian Ungermann[b], and Rutilio A. Fratti[a]
[a]Department of Biochemistry, University of Illinois at Urbana–Champaign, Urbana, IL 61801; [b]Biochemistry Section, Department of Biology/Chemistry, University of Osnabrück, 49076 Osnabrück, Germany

ABSTRACT Maturation of organelles in the endolysosomal pathway requires exchange of the early endosomal GTPase Rab5/Vps21 for the late endosomal Rab7/Ypt7. The Rab exchange depends on the guanine nucleotide exchange factor activity of the Mon1-Ccz1 heterodimer for Ypt7. Here we investigate vacuole binding and recycling of Mon1-Ccz1. We find that Mon1-Ccz1 is absent on vacuoles lacking the phosphatidic acid phosphatase Pah1, which also lack Ypt7, the phosphatidylinositol 3-kinase Vps34, and the lipid phosphatidylinositol 3-phosphate (PI3P). Interaction of Mon1-Ccz1 with wild-type vacuoles requires PI3P, as shown in competition experiments. We also find that Mon1 is released from vacuoles during the fusion reaction and its release requires its phosphorylation by the type 1 casein kinase Yck3. In contrast, Mon1 is retained on vacuoles lacking Yck3 or when Mon1 phosphorylation sites are mutated. Phosphorylation and release of Mon1 is restored with addition of recombinant Yck3. Together the results show that Mon1 is recruited to endosomes and vacuoles by PI3P and, likely after activating Ypt7, is phosphorylated and released from vacuoles for recycling.

INTRODUCTION

Eukaryotic cells are compartmentalized by membrane-bound organelles, leading to the specific localization of proteins and enzymatic reactions. Cargo is packaged into vesicles at donor organelles and transported to acceptor membranes, culminating in a fusion event that is regulated by organelle-specific Rab GTPases, their effectors, and soluble *N*-ethylmaleimide–sensitive factor attachment protein receptor (SNARE) proteins. It was discovered that organelles can mature from early to late stages, characterized in part by sequential recruitment and activation of Rab proteins (Rivera-Molina and Novick, 2009). In a general model it is now believed that Rab GTPase guanine nucleotide exchange factors (GEFs) regulate Rab delivery to specific membranes (Gerondopoulos et al., 2012). In the endocytic pathway, early endosomes recruit and activate Rab5/Ypt21 through the function of the GEF Vps9/Rabex-5 (Hama et al., 1999; Esters et al., 2001). GTP-bound Rab5 is the active form of the protein and can recruit early endosome–specific effectors, including the tethering factor EEA1 and rabaptin-5 (Stenmark et al., 1995; Christoforidis et al., 1999; McBride et al., 1999). Rabaptin-5 inhibits the GTPase activity of Rab5, prolonging the "on" state of Rab5 (Rybin et al., 1996). In *Caenorhabditis elegans*, Rab5-positive endosomes recruit SAND-1/Mon1, the GEF for the late endosome and lysosome–specific Rab7. Recruitment of SAND-1 occurs in a phosphatidylinositol 3-phosphate (PI3P)–dependent manner (Poteryaev et al., 2010). SAND-1 physically interacts with the Rab5 GEF Rabex-5, leading to its displacement. Subsequently, Rab5 hydrolyzes GTP to become the inactive GDP-bound form, which is then lost from the endosome. However, the constitutively active Rab5[Q79L] mutant is resistant to SAND-1–mediated inactivation, indicating that
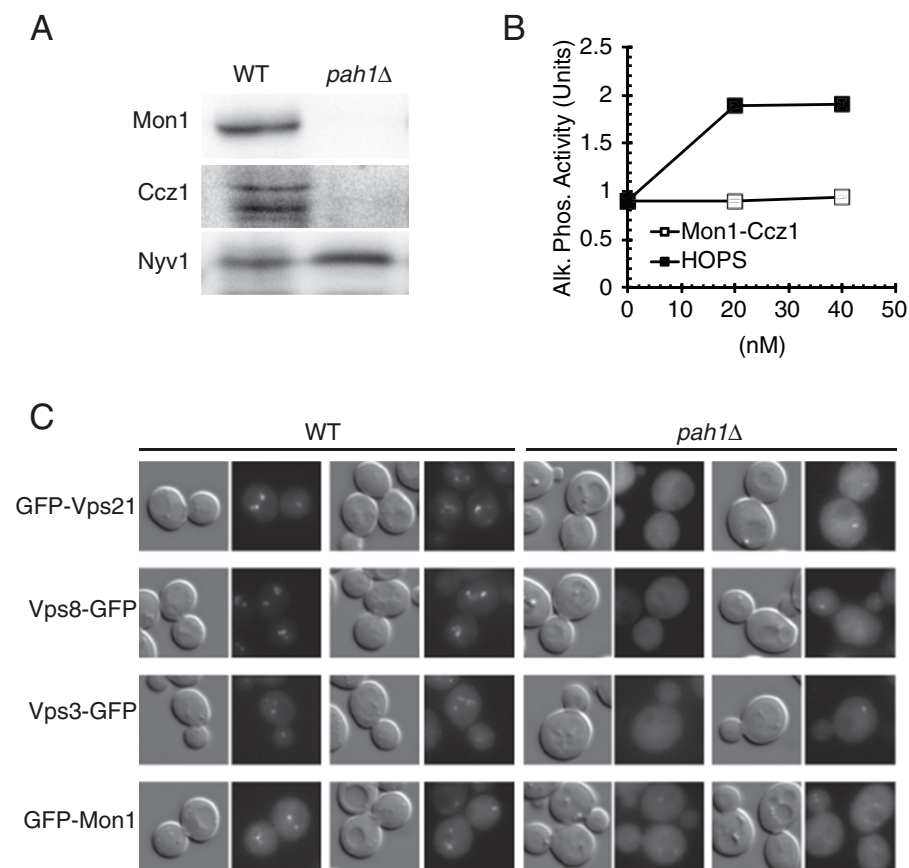
FIGURE 1: Mon1, Vps21, and CORVET subunits are mislocalized in *pah1Δ* cells. (A) Vacuoles were isolated from WT and *pah1Δ* strains and incubated under fusion conditions for 0 or 60 min. At the end of the incubation, membranes were resolved by 10% SDS–PAGE and analyzed by immunoblotting for the distribution of Mon1, Ccz1, and Nyv1. (B) Fusion reactions with *pah1Δ* vacuoles were incubated with buffer or supplemented with exogenous HOPS or Mon1-Ccz1 complex at the indicated concentrations in the presence of fusion reaction buffer and 1 mM GTP. Fusion was measured after 90 min at 27°C. Data represent mean values ± SEM. (C) WT and *pah1Δ* strains were transformed with plasmids encoding GFP gene fusions to *VPS21*, *VPS8*, *VPS3*, and *MON1*. Cells were analyzed by differential interference contrast and fluorescence microscopy.

in vitro homotypic fusion (Wang *et al.*, 2003). The defect in fusion was mapped to the Ypt7-dependent tethering stage, and deleting Mon1 or Ccz1 prevented the interaction between HOPS and SNAREs. Of interest, it was observed that Mon1 was released from vacuoles through an ATP-dependent mechanism. Furthermore, released Mon1 displayed an electrophoretic mobility shift, as detected by immunoblotting, suggesting that Mon1 undergoes posttranslational modification as part of the release mechanism (Wang *et al.*, 2003).

In a previous study, we showed that deletion of *PAH1* blocked the recruitment of Ypt7, the HOPS subunit Vps39, the phosphatidylinositol (PI) 3-kinase Vps34, and its product PI3P to the vacuoles (Sasser *et al.*, 2012). Pah1 is a soluble phosphatidic acid phosphatase that generates diacylglycerol during the fusion reaction. PI3P is produced by Vps34 in vacuolar fractions and plays important roles in the formation of membrane microdomains, SNARE function, and actin dynamics (Schu *et al.*, 1993; Boeddinghaus *et al.*, 2002; Fratti *et al.*, 2004; Thorngren *et al.*, 2004; Karunakaran *et al.*, 2012). Taking the results together, we hypothesized that Pah1 activity leads to the recruitment of the Mon1-Ccz1 complex and maturation of vacuoles via PI3P, culminating in Ypt7 recruitment. In this study, we show that Mon1-Ccz1 is excluded from *pah1Δ* vacuoles and that Mon1-Ccz1 associates with vacuoles in a PI3P-dependent manner. Of importance, we find that Mon1 is released from vacuoles after phosphorylation by the casein kinase Yck3 as part of a putative recycling mechanism.

RESULTS

Mon1 and Ccz1 are absent from *pah1Δ* vacuoles

In a previous study, we found that deletion of *PAH1* causes severe deficiency of multiple factors to vacuole membranes (Sasser *et al.*, 2012). The PI 3-kinase Vps34, the HOPS subunit Vps39, and the Rab GTPase Ypt7 were severely depleted or completely absent from *pah1Δ* vacuoles. Because Vps39 and Vps34 are linked to the early endosome Rab5/Vps21 and the late endosome/lysosome Rab7/Ypt7, we further investigated the effect of Pah1 on Rab conversion. In *C. elegans*, the recruitment of the Rab7 GEF SAND-1 to late endosomes required the presence of PI3P (Poteryaev *et al.*, 2010), even though PI3P depletion did not affect Mon1-Ccz1 localization to endosomes in *Drosophila* tissues (Yousefian *et al.*, 2013). Because *pah1Δ* vacuoles lack Vps34 and its product PI3P, we examined whether the membrane association of the SAND-1 homologue Mon1 would be altered on these mutant vacuoles. Using isolated vacuoles from wild-type and *pah1Δ* yeast strains, we found that Mon1 was largely absent from *pah1Δ* vacuoles (Figure 1A). As expected, the Mon1-interacting Ccz1 was also absent from *pah1Δ* vacuoles. Probing for Nyv1 served as a loading control.

Rab5 must hydrolyze GTP before it is removed from endosomes. Others have shown that SAND-1 physically interacts with Rab7, leading to its recruitment to maturing phagosomes (Kinchen and Ravichandran, 2010). In addition, mutations in SAND-1, Ccz1, or Rab7 lead to an arrested maturation characterized by the retention of high levels of Rab5 and PI3P on phagosomes containing apoptotic corpses.

In *Saccharomyces cerevisiae* the Ypt7 GEF was initially believed to be the Vps39 subunit of the heterohexameric homotypic fusion and vacuole protein-sorting (HOPS) complex (Wurmser *et al.*, 2000; Ostrowicz *et al.*, 2010). However, Rytka and colleagues later reported that Ypt7 GEF activity was controlled by the protein Ccz1 (Kucharczyk *et al.*, 2001). More recent studies demonstrated that the Mon1-Ccz1 dimer is the definitive GEF for Ypt7 (Nordmann *et al.*, 2010), thus nicely explaining the intriguing in vivo data obtained in *C. elegans* (Kinchen and Ravichandran, 2010; Poteryaev *et al.*, 2010). Initially, the Mon1-Ccz1 complex was found to function in various autophagy pathways (Wang *et al.*, 2002). In addition, deletion of either Mon1 or Ccz1 leads to vacuole fragmentation, a hallmark of defective vacuole homeostasis. Vacuoles lacking Mon1 or Ccz1 are blocked in

We next asked whether the addition of purified HOPS or Mon1-Ccz1 would rescue the fusion defect of pah1Δ vacuoles. In Figure 1B we show in vitro fusion reactions of pah1Δ vacuoles in the presence or absence of purified HOPS and Mon1-Ccz1. We find that Mon1-Ccz1 alone does not affect the fusion of pah1Δ vacuoles. This is likely due to the absence of Ypt7 on isolated vacuoles. However, the addition of purified HOPS to pah1Δ reactions can stimulate fusion at 20–40 nM by twofold. This suggests that HOPS has the ability to tether vacuoles in the absence or at reduced levels of Ypt7. The ability of HOPS to stimulate the fusion of pah1Δ vacuoles is likely due to tethering vacuoles through interactions with SNAREs and other phosphoinositides (Stroupe et al., 2006).

The recruitment of Mon1-Ccz1 to endosomes is believed to lead to inactivation of the early endosome Rab Vps21, followed by recruitment and activation of Ypt7. However, the physical exchange of these two Rabs is difficult to directly observe. Other studies showed that overexpression of BLOC-1, which recruits the Vps21 GTPase-activating protein (GAP) Msb3 to endosomes, does not lead to the loss of the early Rab (John Peter et al., 2013). In addition, deletion of MSB3 causes accumulation of Vps21-GTP and its effector Vps8 at the vacuole along with Ypt7, indicating that loss of Vps21 is not required for acquisition of Ypt7 (Lachmann et al., 2012). Similarly, cells harboring the active Vps21^{Q66L} mutant, which is enriched on vacuoles, causes a shift of Mon1 to the vacuole fraction. Along with the exchange of Rabs, it is believed that class C core vacuole/endosome tethering (CORVET) complex, an early endosome-tethering complex, would be exchanged for the late endosomal–tethering complex HOPS (Peplowska et al., 2007). CORVET and HOPS share a core class C heterotetramer composed of Vps11, Vps16, Vps18, and Vps33. The CORVET complex also contains Vps3 and Vps8 as Rab-binding subunits, whereas HOPS contains Vps39 and Vps41, respectively. Thus we imagined that lack of Mon1 and Ypt7 on pah1Δ vacuoles would be accompanied by accumulation of Vps21 and CORVET subunits. To test this, we examined in vivo localization of fluorescently tagged proteins. In Figure 1C, we show that deletion of PAH1 leads to redistribution of various factors from punctate staining to dispersed cytoplasmic staining. Vps21 and the CORVET subunits Vps3 and Vps8 show decreased punctate staining in pah1Δ cells relative to wild-type yeast, indicating that sorting to endosomes is altered. We originally predicted that pah1Δ vacuoles would be enriched in Vps21 and CORVET subunits. Instead, we find that Vps21 and CORVET are missing from the vacuole and reduced on endosomes. This suggests that Pah1 might play a role throughout the endolysosomal pathway. When GFP-Mon1 distribution was examined in vivo, we observed a decrease in punctate staining, illustrating that the PAH1 deletion had negative effects on endosomes, as well as on vacuoles.

Mon1 requires PI3P for its retention on vacuoles

Other investigators showed that the Mon1 homologue SAND-1 requires the presence of PI3P for its recruitment to endosomal membranes (Poteryaev et al., 2010). Because pah1Δ vacuoles lack the PI 3-kinase Vps34, as well as newly synthesized PI3P, we hypothesized that the absence of Mon1 from pah1Δ vacuoles was due in part to its inability to bind vacuoles in the absence of PI3P. To examine the role of PI3P in Mon1 binding to vacuoles, we used wild-type vacuoles that produce PI3P and performed release assays using the high-affinity PI3P ligand FYVE or the PI3P 3-phosphatase MTM-1 (Gillooly et al., 2000; Taylor et al., 2000). Fusion reactions were treated with buffer or dose curves of FYVE or MTM-1. After incubation on ice for 5 min, the membranes and soluble fractions were separated by centrifugation and probed by immunoblotting for Mon1. We found that

Mon1 was displaced from the vacuole membrane fraction by the FYVE domain in a dose-dependent manner (Figure 2A), suggesting that Mon1 binding required PI3P. Similarly, we found that treatment with MTM-1 caused a dose-dependent release of Mon1 (Figure 2B). We confirmed that our recombinant MTM-1 was active by using a malachite green phosphatase assay as described by others (Carter and Karl, 1982; Maehama et al., 2000; Figure 2C). We next used purified yeast actin to examine whether the release of Mon1 seen earlier was due to the role of PI3P or nonspecific protein excess. We found that adding exogenous actin did not result in the release of Mon1, indicating that the effects of FYVE and MTM-1 were not due to an effect of excess protein in the reaction (Figure 2D). Together these experiments show that like SAND-1 in C. elegans, the yeast homologue Mon1 requires PI3P for stable association with membranes. This is consistent with in vitro studies showing that purified Mon1 binds to liposomes containing PI3P (Cabrera et al., 2014).

In a previous study we found that treating vacuoles with the drug propranolol inhibited fusion by inhibiting the PA phosphatase activity of Pah1 (Sasser et al., 2012). Because deletion of PAH1 resulted in the exclusion of Mon1 (Figure 1A), as well as of Vps34, we tested whether propranolol would lead to an increase in Mon1 release from vacuoles. Figure 2E shows a dose–response curve of propranolol and Mon1 release. These concentrations of propranolol were previously shown to inhibit fusion (Sasser et al., 2012). We observed a significant increase in Mon1 release in a dose-dependent concentration of propranolol. This suggested that newly formed PI3P might stabilize the interaction between Mon1 and the vacuoles. However, propranolol could also have indirect effects that result in Mon1 release independent of PI3P synthesis. Vacuoles acquire PI3P by two modes. PI3P is made on endosomes (Gillooly et al., 2000), which can traffic to the vacuole and transfer the lipid upon fusion. In addition, vacuole-associated Vps34 makes new PI3P on the vacuole surface during the homotypic fusion reaction (Thorngren et al., 2004). To ask whether new rounds of PI3P synthesis play a role in Mon1 association with vacuoles, we treated fusion reactions with the PI 3-kinase inhibitor LY294002. We found that treating vacuoles with LY294002 had a minimal effect on Mon1 retention (Figure 2F), suggesting that the starting levels of PI3P were sufficient for Mon1 vacuole binding. This is consistent with the notion that Mon1 arrives at the vacuole via endolysosomal trafficking. This is also consistent with previous findings showing that inhibiting PI 3-kinase activity with wortmannin had no effect on membrane fusion (Boeddinghaus et al., 2002).

To further examine the role of PI3P in vacuole maturation, we compared the protein profile of vps34Δ and wild-type vacuoles. We found that vps34Δ vacuoles were severely depleted in many components of the fusion machinery, including the SNAREs Vam3 and Vam7, the HOPS subunits Vps11 and Vps18, and Mon1, Ccz1, and Ypt7 (Figure 2G). However, not all proteins were depleted on vps34Δ vacuoles, as shown by the wild-type levels of Sec18 and actin. Although this mutant shared several protein deficiencies versus pah1Δ vacuoles, it should be noted that vps34Δ vacuoles were more severely affected. This is consistent with the fact that pah1Δ was not identified as a vacuolar protein sorting mutant.

Mon1 is released from the vacuole after phosphorylation

Previously, Klionsky and colleagues found that Mon1 was released from the membrane after the addition of ATP (Wang et al., 2003). To further characterize the observed release reaction, we performed time-course experiments to monitor the release of Mon1 from vacuoles. Fusion reactions were incubated at 27°C from 0 to 60 min, after which the membranes were separated from the supernatant by
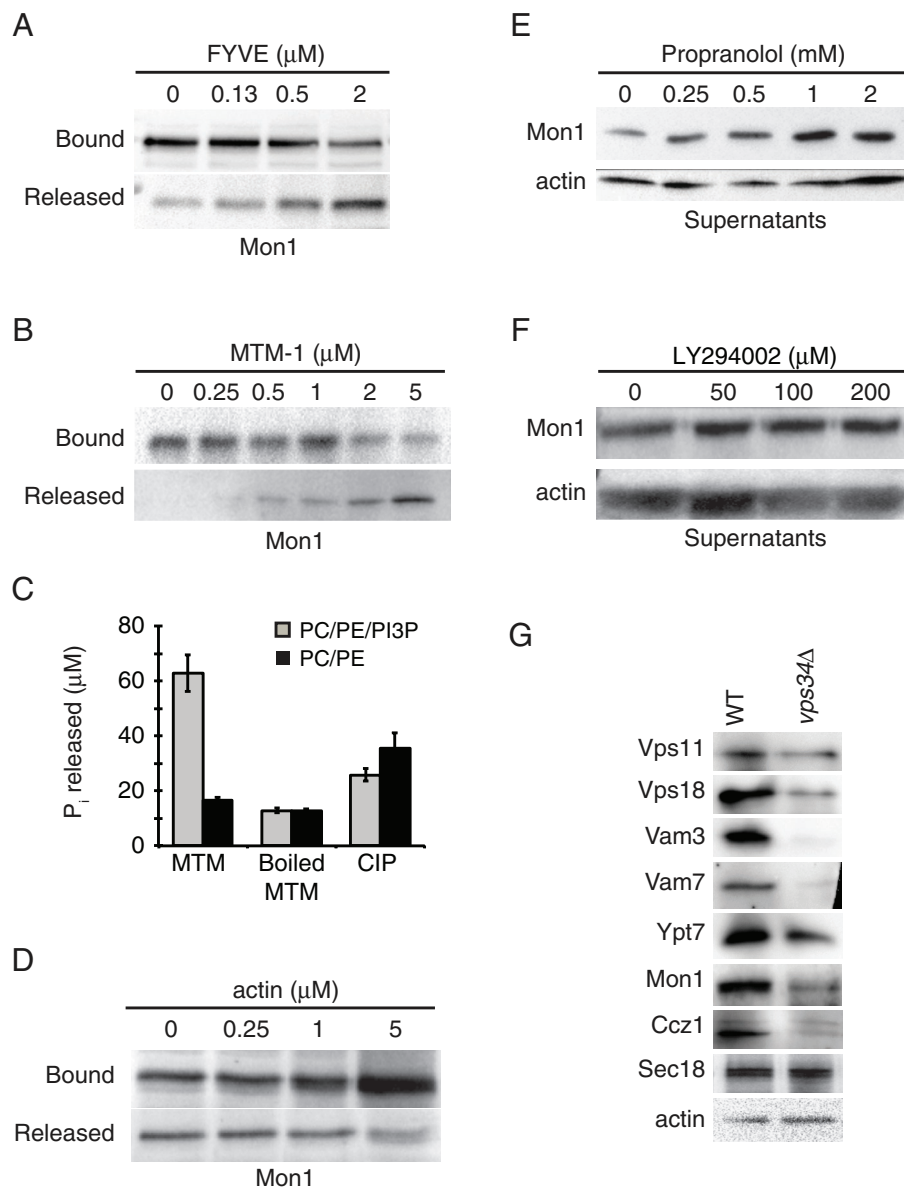
FIGURE 2: Mon1-Ccz1 interacts with vacuolar membranes in a PI3P-dependent manner. Fusion reactions containing WT vacuoles were incubated with buffer or a dose curve of GST-FYVE (A) or MTM-1 (B) for 5 min on ice. The reactions were separated into membrane (bound) and supernatant (released) fractions and resolved by 10% SDS–PAGE. Immunoblot analysis was carried out using antisera against Mon1. (C) Quantitation of MTM-1 activity using a malachite green phosphatase activity assay. Calf intestinal phosphatase (CIP) was used as control. (D) As a control for Mon1 release in the presence of exogenous proteins, fusion reactions were incubated with a dose curve of purified yeast actin. Mon1 binding was determined by fractionation of membrane-bound and soluble Mon1. (E) The effect of blocking PA phosphatase activity on Mon1 retention was examined by incubating fusion reactions with propranolol for 60 min at 27°. Afterward, the released Mon1 was collected and examined by immunoblotting. Actin served as a loading control. (F) The effect of Vps34 activity on Mon1 release was tested by incubating fusion reactions with the PI 3-kinase inhibitor LY294002 for 60 min at 27°C. Released Mon1 was determined by immunoblotting. (G) Vacuoles from WT and *vps34Δ* yeast were isolated and examined by immunoblotting using antibodies against the indicated proteins.

centrifugation. We found that very little Mon1 was present in the supernatant at the beginning of the fusion reaction, and that Mon1 accumulated in the supernatant over time (Figure 3A). Ccz1 accompanied the release of Mon1, as expected for the heterodimer. As controls, we probed for the release of HOPS subunit Vps41, actin,

and Ypt7. Some Vps41 was released over time, whereas Ypt7 remained in the membrane fraction, indicating that the release of Mon1 was a result of its activity during the fusion process and not due to membrane lysis. Actin served as loading control for both pellet and supernatant fractions.

To identify the requirements for Mon1 release during fusion, we used a panel of well-characterized inhibitors that block fusion at various stages of the pathway. We used anti-Sec17 immunoglobulin G (IgG) to inhibit the priming stage. Ypt7-dependent tethering was inhibited with anti-Ypt7 IgG or the GTPase-activating factor Gyp1. Docking was inhibited with antibodies against the SNARE Vti1 or the HOPS subunit Vps11. Reactions were incubated for 0 or 60 min, and released Mon1 was collected by centrifugation. We found that the untreated control released Mon1 in a time-dependent manner, whereas blocking SNARE priming with anti-Sec17 reduced Mon1 release between the two time points (Figure 3B). This suggests that Mon1 release is linked to the start of the fusion cascade. Blocking Vti1 had little effect on Mon1 release, suggesting that SNARE pairing occurs after Mon1 activity is completed. Of interest, blocking Ypt7 directly with antibody or converting it to the GDP-bound state with Gyp1 accelerated Mon1 release. We suspect that the antibody directly inhibited the interaction between Mon1 and Ypt7. We also found that blocking HOPS with anti-Vps11 antibody accelerated release. This was likely due to disruption of direct interaction between Mon1 and the HOPS complex (Wang *et al.*, 2003; Nordmann *et al.*, 2010; Poteryaev *et al.*, 2010). In fact, the effects of anti-Ypt7 and Gyp1 could also be linked to disturbing the HOPS–Mon1 interaction, as previous reports showed that both the antibody and GAP resulted in the release of HOPS from the membrane (Eitzen *et al.*, 2000; Price *et al.*, 2000; Brett *et al.*, 2008).

The nucleotide-binding state of Ypt7 affects Mon1 release

Because Rab GTPases undergo conformational changes when interacting with GEFs, we hypothesized that release of Mon1 was tied to conformational changes in Ypt7 upon binding GTP. To test this, we used point mutations of Ypt7 that affect GTP/ GDP binding (Eitzen *et al.*, 2000). Based on conserved residues in the Rab family, the Ypt7[Q68L] mutant is believed to be locked in the GTP-bound stage, maintaining an active state. The Ypt7[T22N] mutant is believed be a nucleotide empty mutant remaining in the inactive state. We used reactions containing wild-type (WT) or mutant Ypt7 and examined Mon1 release by immunoblotting. We hypothesized that Mon1 is
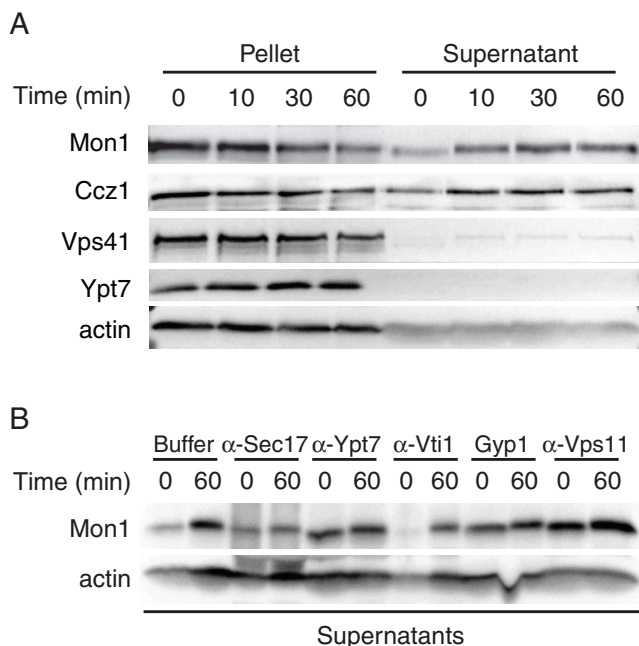
A

B

FIGURE 3: Mon1 is released from vacuoles during the fusion reaction. (A) Fusion reactions containing WT vacuoles were incubated at 27°C for 0, 10, 30, or 60 min. After incubation the membrane fraction was isolated by centrifugation. The membrane fraction and supernatants were examined for the release of Mon1 from vacuoles. Immunoblots were performed using antibodies against Mon1, Ccz1, Vps41, Ypt7, and actin. (B) Release of Mon1 was examined in fusion reactions treated with inhibitors that targeted different stages of fusion. Reactions were treated with buffer, 67 μg/ml anti-Sec17, 8 μg/ml anti-Ypt7, 50 μg/ml anti-Vps11, 27 μg/ml anti-Vti1, or 0.5 μM Gyp1-46 and incubated for 60 min at 27°C. Mon1p distribution was examined as described in A.

recycled from the vacuole after Ypt7 activation and that a block in activation would alter Mon1 membrane release. We found that vacuoles containing Ypt7^{Q68L} released more Mon1 relative to WT organelles (Figure 4, A and B). In contrast, vacuoles harboring Ypt7^{T22N} did not release Mon1 even after 60 min of incubation. These data indicate that release of Mon1 is directly tied to conformational changes that Ypt7 undergoes during nucleotide exchange. Our findings are consistent with previous studies by Horazdovsky and colleagues that showed augmented binding between the inactive Rab5 homologue Vps21^{S21N} and its GEF Vps9 (Hama et al., 1999). These data are also in keeping with the enhanced binding of Rab5^{S34N} with its GEF Rabex-5 (Zhu et al., 2009). Taken together, it is apparent that the conformation of Rab GTPases affects interactions with their respective GEFs. As a control, we probed for the presence of Ypt7 on these vacuoles (Figure 4C). We found that both mutations of Ypt7 resulted in a reduction in vacuole association. This could be due to inhibited delivery of GTP-Ypt7^{Q68L} by GDP dissociation inhibitor (GDI) and by enhanced GDI removal of GDP-Ypt7^{T22N}. We also examined the release of the HOPS subunit Vps41 and found that vacuoles containing Ypt7^{T22N} were nearly devoid of the protein (Figure 4D). This is consistent with the exclusive association of an effector complex such as HOPS with the Rab-GTP form (Brocker et al., 2012). Others also showed reduced binding of HOPS subunits with these Ypt7 mutants (Eitzen et al., 2000; Brett et al., 2008) and Ccz1 (Kucharczyk et al., 2001).

Mon1 is phosphorylated during release

It was previously observed that the soluble form of Mon1 migrated more slowly on SDS–PAGE gels relative to the membrane-bound pool of Mon1 (Wang et al., 2003). We also observed a shift in the previous experiments using 10% SDS–PAGE gels and posited that the observed electrophoretic mobility change might be due to protein phosphorylation. To further distinguish the shift in gel migration, we resolved vacuole extracts using 6% SDS–PAGE. Figure 5A shows that a second, higher–molecular weight Mon1 band appeared only in the presence of ATP, suggesting that Mon1 was phosphorylated during the fusion reaction. On the basis of comparison with the membrane release data presented in Figure 3, we hypothesize that Mon1 modification occurs before membrane release. To test the effect of Mon1 modification on membrane association, we performed membrane fractionation assays and found that the supernatant contained only the upper Mon1 band, indicating that phosphorylation might trigger release from vacuoles (Figure 5B). In addition, release of Mon1 from the membrane only occurred in the presence of ATP, further suggesting that protein modification leads to the dissociation from the vacuole. Of interest, modified Mon1 was also present in the pellet fraction. Thus modification of Mon1 is linked but not sufficient to trigger its release from the membrane, indicating that other factors are likely involved. To determine whether the migration shift was truly due to phosphorylation, we treated reactions with either buffer or calf intestinal phosphatase (Figure 5C). We found that using the phosphatase downshifted the higher–molecular weight band.

Previous studies showed that exogenous recombinant Vam7 can bypass a block in SNARE priming by anti-Sec17 IgG (Merz and Wickner, 2004; Thorngren et al., 2004). To determine whether fusion is required for Mon1 phosphorylation, we blocked fusion reactions with anti-Sec17 IgG in the presence or absence of Vam7 for 0 or 60 min. Control reactions show that Mon1 phosphorylation only occurred in the presence of ATP (Figure 5D). The addition of anti-Sec17 in the presence of ATP did not affect phosphorylation of Mon1, indicating that SNARE priming was not required for its modification. The addition of Vam7, which bypasses the anti-Sec17 block to stimulate fusion, did not alter the amount of phosphorylated Mon1.

Yck3p phosphorylates Mon1p

Studies show that the casein kinase Yck3 phosphorylates the fusion regulators Vps41 and Vam3 (LaGrassa and Ungermann, 2005; Brett et al., 2008; Cabrera et al., 2009). Because this kinase is linked to the fusion machinery, we examined whether Yck3 phosphorylated Mon1 during fusion. To this aim, we used vacuoles from yck3Δ yeast and monitored the relative mobility shift of Mon1. We found that Mon1 remained as a single low–molecular weight form on yck3Δ vacuoles (Figure 6A). As a control, we also monitored Vps41 in these experiments and found that it was not modified on yck3Δ vacuoles, which is in keeping with previous studies. In comparison, wild-type vacuoles exhibited phosphorylation of Mon1 and Vps41. To confirm that Yck3 was directly modifying Mon1, we used recombinant hexahistidine (His$_6$)-Yck3 in complementation experiments. Here yck3Δ vacuoles were incubated in fusion reactions that were treated with buffer or exogenous His$_6$-Yck3. We found that adding His$_6$-Yck3 restored the phosphorylation pattern of Mon1 during fusion, indicating that the kinase directly modified Mon1 during fusion (Figure 6B). In addition, we fractionated these reactions and found that Mon1 was not released from yck3Δ vacuoles and that Mon1 release was restored in the presence of His$_6$-Yck3. Together these data strongly indicate that modification and release of Mon1 from vacuoles
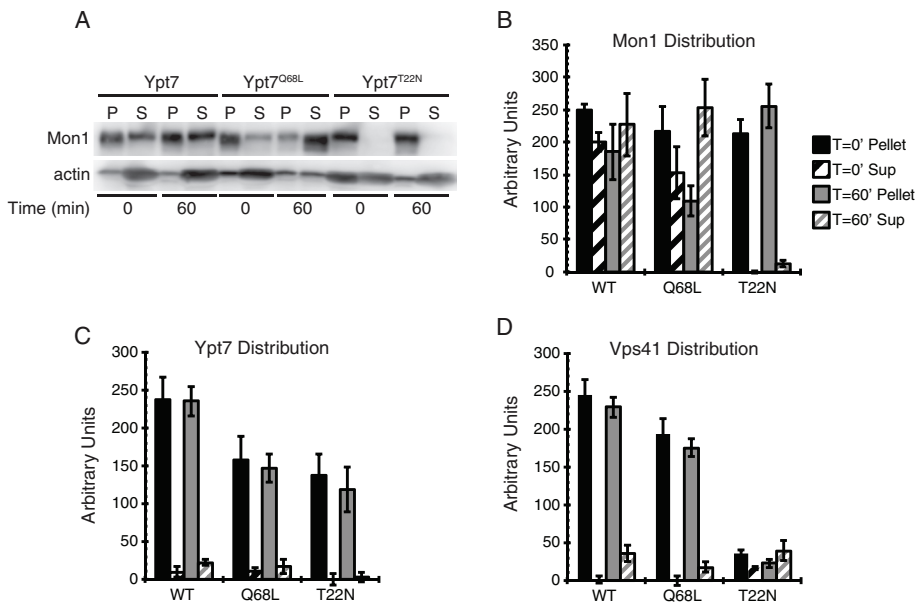
FIGURE 4: The nucleotide-binding state of Ypt7 affected the distribution of Mon1 and binding of HOPS. Fusion reactions were performed using vacuoles that harbor WT, Ypt7^{Q68L}, or Ypt7^{T22N} and incubated for 60 min at 27°C. After incubation the reactions were separated into membrane and soluble fractions as described. Membrane and supernatant fractions were examined by immunoblotting using antibodies against (A, B) Mon1, (C) Ypt7, and (D) Vps41. (A) A representative immunoblot of Mon1 distribution at 0 or 60 min of incubation using the indicated strains. (B–D) Quantitations of three experiments. Data represent mean values ± SEM.

during fusion was due to Yck3 function. It is also important to note that phosphorylated Mon1 was present on the membrane fraction of wild-type vacuoles. This suggests that phosphorylation is not the only cause of membrane release. It is likely that other step(s) occur after Mon1 phosphorylation that leads to the ultimate release of the protein. To examine whether Yck3 directly phosphorylated Mon1, we performed an in vitro assay using purified Mon1 and recombinant Yck3. Figure 6C shows that Yck3 directly phosphorylates purified Mon1 in the absence of other vacuolar components. Note that the amount of in vitro–phosphorylated Mon1 is reduced in comparison to what is seen using whole-vacuolar reactions. One possibility for the difference could be due to conformational changes that occur on the membrane in the presence of Ypt7, HOPS, and PI3P. This is only a hypothesis and will be tested in future studies. Finally, we asked whether inhibiting Ser/Thr kinases during the fusion reaction would alter release of Mon1. We performed fusion reactions in the presence of increasing amounts of staurosporine, a broad-spectrum protein kinase inhibitor. We found that increasing amounts of staurosporine correlated with increased retention of Mon1 on the membrane fraction (Figure 6D). This is in keeping with our other experiments showing that protein phosphorylation is linked to Mon1 release from the vacuole.

To further examine the link between Mon1 phosphorylation and membrane association, we generated Mon1 mutants that eliminated Yck3 phosphorylation sites (NetPhos, www.cbs.dtu.dk/services/NetPhos/; Scansite, http://scansite.mit.edu/). In one strain, the Mon1 residues S35, T38, T39, S130, S135, and S138 were mutated to Ala (Mon1-6A). A second mutant contained phosphomimetic mutations of the same residues changed to Asp (Mon1-6D). Mutations of these sites to Ala or Asp abolished the mobility shift of Mon1 during fusion reaction, which was identical to the effect of deleting YCK3 (Figure 7A). Because the mutations blocked the electrophoretic shifts seen with phosphorylation, we next asked whether

membrane release was also affected. These experiments were performed in the presence or absence of ATP and observed after 0 and 60 min. As seen before, deletion of YCK3 blocked Mon1 phosphorylation as well as release (Figure 7B). Similarly, Mon1-6A and Mon1-6D remained associated with the vacuoles (Figure 7, C and D). This further demonstrates that Yck3-dependent phosphorylation is required for the release of Mon1 during the fusion reaction. The lack of release of Mon1-6D likely indicates that these phosphomimetic mutations were insufficient in duplicating the phospho-Mon1 phenotype.

To further characterize the Mon1 mutations, we first examined the stability of Mon1 mutants in heterodimers with Ccz1 and found that there was no change in heterodimer formation (Figure 7E). In addition, we performed fusion experiments in which wild-type vacuoles were treated with Gyp1 to convert Ypt7 to the GDP-bound state and to block fusion. Next we added purified Mon1-Ccz1, Mon1-6A-Ccz1, or Mon1-6D-Ccz1 to reactivate Ypt7 and restore fusion. We found that both Mon1 mutants were able to counteract GAP activity and restored fusion as well as the wild-type heterodimer (Figure 7F). This suggests the phosphorylation of Mon1-Ccz1 does not affect the activity of the complex. Finally, we examined vacuole morphology and found that neither mutation affected the vacuole phenotype (Figure 7G). Together these data further support the notion that Mon1 phosphorylation likely occurs downstream of its activity on Ypt7 to ensure release of Mon1-Ccz1 from vacuoles.

DISCUSSION

Nucleotide exchange of Rab GTPases is an integral part of the progression or maturation of organelles. In the early-to-late endosome maturation pathway, the exchange of early-endosomal Rab5/Vps21 for late-endosomal Rab7/Ypt7 depends on the acquisition of Mon1-Ccz1, a heterodimer that functions as the GEF for Ypt7 (Nordmann et al., 2010). Others have found that recruitment of Mon1/SAND-1 interrupts activation of Rab5, allowing for its removal while Rab7 is recruited to the transitioning endosome (Kinchen and Ravichandran, 2010; Poteryaev et al., 2010; Gerondopoulos et al., 2012). In SAND-1–knockdown cells, Rab5 remains active, leading to enlarged endosomes. In C. elegans this mechanism depends on the regulatory lipid PI3P, and depletion of the lipid leads to inhibition of organelle maturation (Poteryaev et al., 2010). In a previous study we found that deletion of the phosphatidic acid phosphatase Pah1 causes arrest in vacuole maturation that is characterized by exclusion of Ypt7 (Sasser et al., 2012). This is accompanied by reduction in the PI 3-kinase Vps34 and its product PI3P. In addition, the HOPS subunit Vps39, which is linked to Mon1-Ccz1 GEF activity (Nordmann et al., 2010), is sharply reduced relative to the other five HOPS subunits. Thus we hypothesize that Pah1 creates the environment that is favorable for Mon1-Ccz1 activity.

In this study we examined our hypothesis and monitored the membrane retention of Mon1 during vacuole fusion. In our experiments, we found that the amount of Mon1-Ccz1 was severely reduced on pah1Δ vacuoles, suggesting that Pah1 activity indirectly
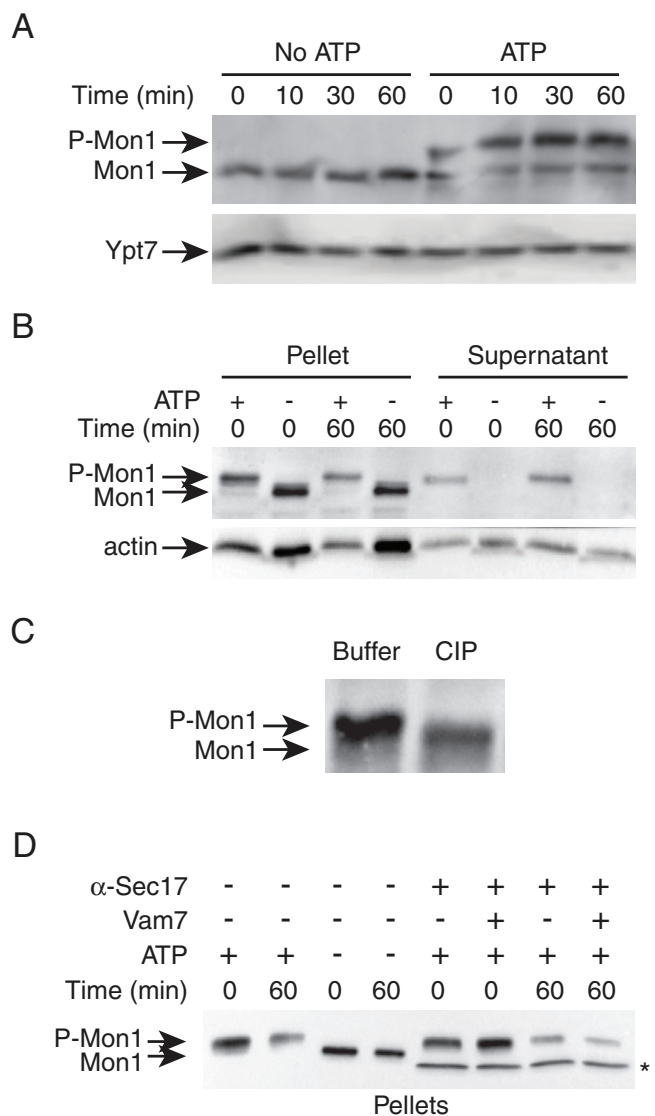
FIGURE 5: Mon1 is phosphorylated before release. (A) Fusion reactions were incubated for the indicated times at 27°C and resolved on 6% SDS–PAGE and probed for Mon1 and Ypt7 by immunoblotting. (B) Reactions were performed as described and separated into membrane and supernatant fractions before being resolved by 6% SDS–PAGE. Mon1p mobility was examined by immunoblot. Actin served as a loading control for pellets and supernatants. (C) A 60-min reaction was performed as described and treated with buffer or calf intestinal phosphatase (CIP) before immunoblotting. (D) The role of fusion activity on Mon1 was examined by blocking fusion with anti-Sec17 IgG. Inhibited reactions were bypassed by the addition of recombinant Vam7 in the indicated lanes. Controls lacking anti-Sec17 were performed in the presence or absence of ATP to detect the electrophoretic mobility shift of modified Mon1. After incubation at 27°C, the membranes and supernatants were separated, and the membrane-bound fraction of Mon1 was detected by immunoblotting. Asterisk Indicates the cross reaction of IgG heavy chain.

FIGURE 6: Yck3 phosphorylates Mon1 during the fusion reaction. (A) Fusion reactions were performed using vacuoles purified from WT and *yck3Δ* strains. The fusion reactions were incubated at 27°C for the indicated times and processed for immunoblotting using antibodies against Mon1 and Vps41. (B) Fusion reactions containing *yck3Δ* vacuoles were performed as described in the presence of buffer or 6 µM recombinant His$_6$-Yck3. After incubation the reactions were separated into membrane and supernatant fractions and processed for immunoblotting of Mon1p. Vam3 distribution was used as a control for the separation of soluble and membrane-bound proteins. (C) In vitro phosphorylation assays of purified Mon1 and recombinant Yck3 were run in the presence or absence of ATP. Phosphorylated Mon1 was detected by immunoblotting. (D) To test whether inhibiting protein kinase activity during the fusion reaction would affect Mon1 distribution, staurosporine was added at the indicated concentrations. After incubation, the membrane-bound fraction of Mon1 was examined by immunoblotting.

affects Mon1-Ccz1 recruitment to vacuoles. This further suggests that Pah1 indirectly interferes with Rab conversion and the transition from early to late endosomes. Part of the regulation of Mon1 binding was due to lack of PI3P on vacuoles. We further characterized the connection between Mon1 vacuole binding and PI3P by competing Mon1 from the vacuoles with the high-affinity ligand FYVE or modifying the
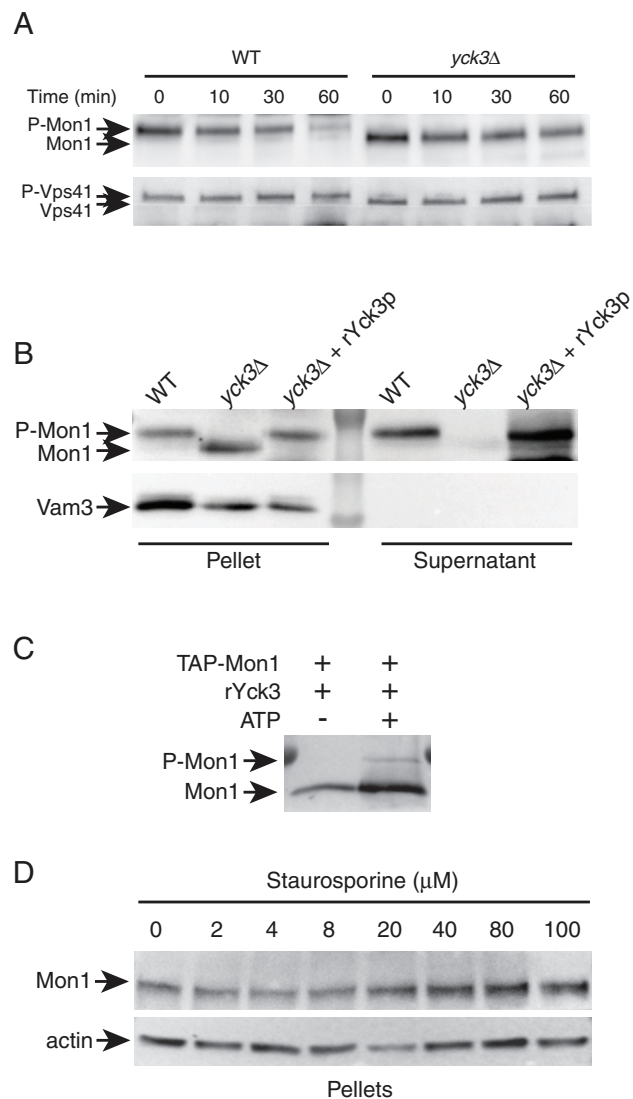
lipid with the phosphatase MTM-1. PI3P not only stabilizes Mon1 and its interaction partner Ccz1 on membranes, but it also stimulates Mon1-Ccz1 GEF activity (Cabrera *et al.*, 2014). The link between GEF activity and phosphoinositides is not unique to the vacuole model. Others have shown that the Sec4 GEF Sec2 functions in Rab cascade in a PI4P-regulated manner (Mizuno-Yamasaki *et al.*, 2010).
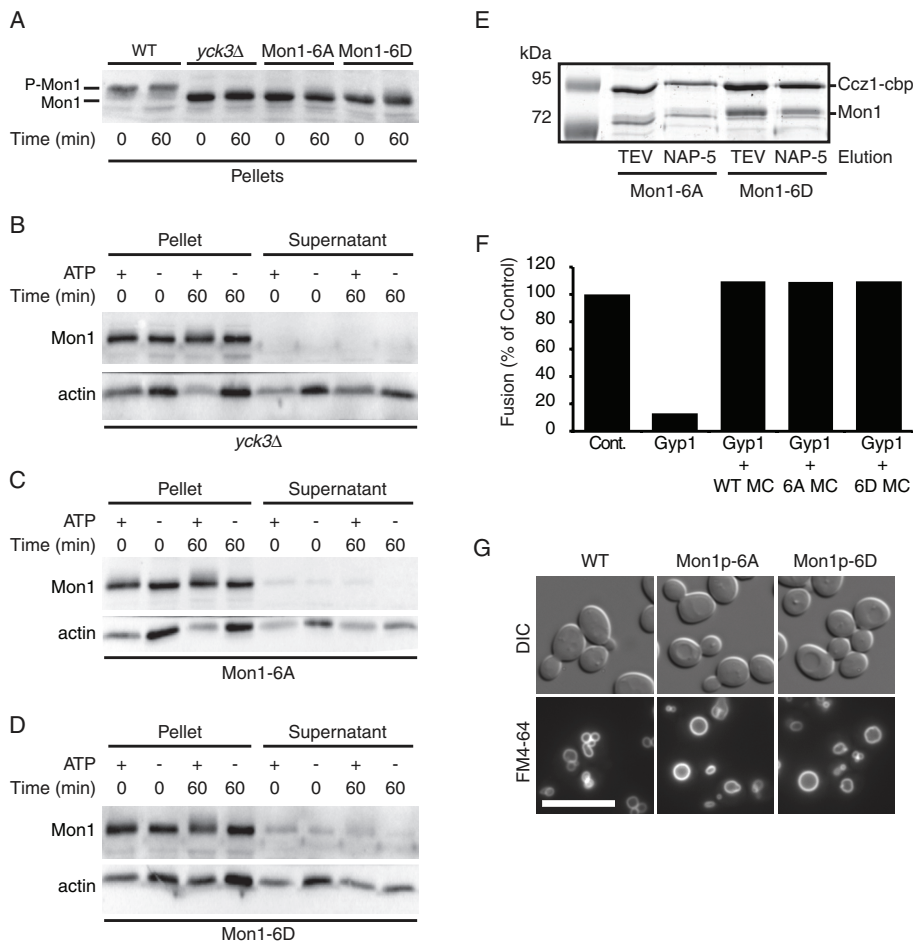
FIGURE 7: Mutations that abolish Mon1p phosphorylation by Yck3p prevent its mobility shift and release on vacuoles. (A) Fusion reactions were performed using vacuoles purified from WT, yck3Δ, Mon1-6A, or Mon1-6D strains and incubated at 27°C for the indicated times. Mon1 mobility was examined by resolving with 6% SDS–PAGE and immunoblotting using antibody against Mon1. Mon1 release was examined using vacuoles from yck3Δ (B), Mon1-6A (C), and Mon1-6D (D). Fusion reactions were incubated for 0 or 60 min in the presence or absence of ATP. Reactions were separated into pellet and supernatant fractions and resolved by 6% SDS–PAGE. Mon1 distribution was detected by immunoblotting. (E) Mon1-Ccz1 heterodimers were isolated from strains containing Mon1-6D and Mon1-6A. Complexes were resolved by SDS–PAGE and stained with Coomassie blue. Samples eluted with TEV protease were run next to samples after buffer exchange using NAP-5 columns. (F) WT fusion reactions were blocked with 0.5 µM Gyp1. Fusion was rescued with the addition of purified wild-type Mon1-Ccz1 (MC) heterodimer. Parallel reactions were treated with buffer or purified heterodimers containing Mon1-6A (6A MC) or Mon1-6D (GD MC). (G) Vacuole morphology of WT, Mon1-6D, and Mon1-6A was examined by FM4-64 staining. Bar, 10 µm

While investigating Mon1 binding to membranes, we found that Yck3 phosphorylated Mon1 and that its modification leads to release of phospho-Mon1 from the membrane. The release of Mon1 was blocked when Yck3 was absent or when the casein kinase phosphorylation sites on Mon1 were mutated. Although little is known about the regulation of GEF activity, there are several reports that show how GEF phosphorylation affects function. For example, during hyphal growth of the opportunistic pathogenic yeast *Candida albicans* the Rab Sec4 is activated by its GEF, Sec2. Localization of Sec2 to the tip of polarized hyphal growth requires phosphorylation by the cyclin-dependent kinase Cdc28 (Bishop *et al.*, 2010). Others have shown that in Mast cells the RhoA GTPase is activated by GEF-H1, which is phosphorylated by the kinase Pak2 to turn off RhoA-dependent signaling and fusion at the plasma membrane. Phospho-

GEF-H1 is released from the RhoA sites and relocalizes to microtubules. In the absence of Pak2, GEF-H1 continuously reactivates RhoA, leading to augmented signaling and fusion (Kosoff *et al.*, 2013). Another example is found in the regulation of Rac1 in the outgrowth of cortical neurons. In embryonic rat cortex the Rac1 GEF Trio is phosphorylated by the Src family kinase Fyn to inhibit Trio activity (Degeer *et al.*, 2013). The inability of Fyn to phosphorylate Trio leads to continued Rac1 function and dysregulated axon outgrowth.

Together these examples illustrate that GEF phosphorylation plays an important role in regulating small-GTPase activity. In addition, modification and redistribution of phosphorylated GEFs is likely part of a recycling pathway. In the case of Mon1, it is thus possible that its phosphorylation by Yck3 serves to recycle Mon1 from the vacuolar surface. However, full recycling would require a dephosphorylation step that occurs in the cytosol, which needs to be explored in future studies.

Yck3 plays additional roles in regulating vacuole fusion, including the phosphorylation of the HOPS subunit Vps41 in adaptor protein-3–dependent *trans*-Golgi network–to-vacuole trafficking, as well as in endosome-to-lysosome and homotypic vacuole fusion (LaGrassa and Ungermann, 2005; Cabrera *et al.*, 2009, 2010). In the absence of Yck3, Vps41 accumulates on puncta adjacent to the vacuole membrane or on the vacuole itself. Deletion of *YCK3* also leads to augmented vacuole fusion, whereas excess Yck3 inhibits fusion (LaGrassa and Ungermann, 2005). Of interest, phosphorylated Vps41 is partially released from vacuoles, which is consistent with our results showing release of phospho-Mon1. Conversely, Vps41 was retained on the vacuole on *yck3Δ* vacuoles, which is again similar to results showing that Mon1 is retained on *yck3Δ* vacuoles. The phosphomutants of Mon1 allowed us to analyze the exclusive effect of Yck3 activity in the

Mon1-Ccz1 complex or Vps41, and in fact we observed that Vps41 release was slightly enhanced when Mon1-Ccz1 mutants (6A and 6D) are more stably associated with vacuoles. This supports the idea that efficient nucleotide exchange and effector binding to the Rab might require GEF disassociation and release from membranes. Of note, the characterized phosphorylation sites within Mon1 are located outside the identified Mon1-Ccz1 interaction site, which is required for GEF activity (Cabrera *et al.*, 2014). In agreement, mutations in the phosphorylation sites did not affect Mon1-Ccz1 activity.

In summary, our data provide evidence that the Yck3 kinase affects fusion processes at vacuoles at multiple levels and, as shown here, is an important regulator for efficient recycling of the Mon1-Ccz1 complex from vacuoles.

Strain	Genotype	Source	Strain	Genotype	Source
BJ3505	*MATa pep4::HIS3 prb1-Δ1.6R his3–200 lys2–801 trp1Δ101 (gal3) ura3–52 gal2 can1*	Jones *et al.* (1982)	CHY53	BJ3505 *yck3Δ::hphMX4*	Eitzen *et al.* (2000)
DKY6281	*MATα pho8::TRP1 leu2–3 leu2–112 ura3–52 his3-Δ200 trp1-Δ901 lys2–801*	Haas *et al.* (1994)	CHY54	DKY6281 *yck3Δ:: hphMX4*	Eitzen *et al.* (2000)
			CUY2470	BY4732 *CCZ1::TRP1-GAL1pr CCZ1::TAP-URA3 MON1::HIS3MX6-GAL1*	Nordmann *et al.* (2010)
RFY17	BJ3505, *pah1Δ::Kan^r*	Sasser *et al.* (2012)	CUY3009	BJ3505 *mon1::kanMX URA3::pRS406-NOP1-MON1*	This study
RFY18	DKY6281, *pahΔ::Kan^r*	Sasser *et al.* (2012)	CUY6092	BJ3505 *mon1::kanMX URA3::pRS406-NOP1-MON1 S35A T38A T39A S130A S135A*	This study
BY4741	*MATa his3Δ1 leu2Δ0 met15Δ0 ura3Δ0*	EUROSCARF			
BY4732	*MATa his3Δ200 leu2Δ0 met15Δ0 trp1Δ63 ura3Δ0*	EUROSCARF	CUY6093	BJ3505 *mon1::kanMX URA3::pRS406-NOP1-MON1 S35D T38D T39D S130D S135D*	This study
BY4742	*MATα his3Δ1 leu2Δ0 met15Δ0 ura3Δ0*	Open Biosystems (Huntsville, AL)	CUY6197	BY4741 *mon1::kanMX CCZ1::HIS3-GAL1 CCZ1::TAP-Nat-NT2 URA3::pRS406-GAL1-MON1*	This study
BY4742 vps34Δ	BY4742 MATalpha *his3Δ1 leu2Δ0 met15Δ0 ura3Δ0 vps34::KanMX6*	Open Biosystems	CUY6198	BY4741 *mon1::kanMX CCZ1::HIS3-GAL1 CCZ1::TAP-NatNT2 URA3::pRS406-GAL1-MON1 S35A T38A T39A S130A S135 S138A*	This study
BJ3505 (Q68L)	BJ3505 *ypt7::YPT7^Q68L*	Eitzen *et al.* (2000)			
DKY6281 (Q68L)	DKY6281 *ypt7::YPT7^Q68L*	Eitzen *et al.* (2000)	CUY6199	BY4741 *mon1::kanMX CCZ1::HIS3-GAL1 CCZ1::TAP-Nat-NT2 URA3::pRS406-GAL1-MON1 S35D T38D T39D S130D S135D S138D*	This study
BJ3505 (T22N)	BJ3505 *ypt7::YPT7^T22N*	Eitzen *et al.* (2000)			
DKY6281 (T22N)	DKY6281 *ypt7::YPT7^T22N*	Eitzen *et al.* (2000)			

EUROSCARF, European *Saccharomyces cerevisiae* Archive for Functional Analysis, Institute for Molecular Biosciences, Johann Wolfgang Goethe-University Frankfurt, Frankfurt, Germany.

TABLE 1: Yeast strains used in this study.

MATERIALS AND METHODS

Reagents
Reagents were dissolved in PS buffer (20 mM 1,4-piperazinedi-ethanesulfonic acid [PIPES]–KOH, pH 6.8, 200 mM sorbitol). The recombinant proteins glutathione *S*-transferase (GST)–FYVE (Gillooly *et al.*, 2000), His₆-MTM-1 (Taylor *et al.*, 2000), GST-Vam7 (Fratti *et al.*, 2007; Fratti and Wickner, 2007), yeast actin (Karunakaran *et al.*, 2012), His₆-Yck3 (Hickey and Wickner, 2010), and His₆-Gyp1-46 (Wang *et al.*, 2003) were prepared as described and stored in PS buffer with 125 mM KCl. Mon1 and Ccz1 were purified from yeast as a heterodimer as described (Nordmann *et al.*, 2010). HOPS was purified as described (Brocker *et al.*, 2012). Antibodies against Sec17, Ypt7, Vti1, and Vps11 were prepared as described (Mayer *et al.*, 1996; Mayer and Wickner, 1997; Price *et al.*, 2000; Ungermann *et al.*, 1999)

Strains
Vacuoles from BJ3505 and DKY6281 were used for fusion assays (Table 1; Haas *et al.*, 1995). Tester strains lacking *YCK3* or *PAH1* were described previously (Hickey *et al.*, 2009; Sasser *et al.*, 2012). Strains containing *YPT7* mutations were previously described (Eitzen *et al.*, 2000). *MON1* was deleted from strains using a kanMX4 cassette using PCR products amplified from pFA6-kanMX4 with homology flanking the *MON1* coding sequence (Longtine *et al.*, 1998). For

complementation studies of *mon1Δ*, strains were transformed with 2μ plasmids encoding Mon1-6A or Mon1-6D to generate CUF609 and CUY6093. Transformants were selected on complete synthetic media lacking uracil. For fluorescence microscopy experiments, wild-type and *pah1Δ* strains were transformed with plasmids for the expression of green fluorescent protein (GFP)–Vps21 (1324), GFP-Mon1 (1381), Vps3-GFP (3098), or Vps8-GFP (3096; Table 2). Transformants were grown in selective media.

Vacuole isolation and in vitro vacuole fusion
Vacuoles were isolated by floatation as described (Haas *et al.*, 1995). Standard in vitro fusion reactions (30 μl) contained 3 μg each of vacuoles from BJ3505 and DKY6281 backgrounds, fusion reaction buffer (20 mM PIPES-KOH, pH 6.8, 200 mM sorbitol, 125 mM KCl,

Strain	Genotype	Source
3096	pRS415-P$_{NOP1}$-VPS8-GFP	Cabrera *et al.* (2013)
3098	pRS415-P$_{NOP1}$-VPS3-GFP	Cabrera *et al.* (2013)
1381	pRS416-P$_{NOP1}$-GFP-MON1	This study
1324	pRS416-P$_{NOP1}$-GFP-VPS21	This study

TABLE 2: Yeast plasmids used in this study.

5 mM MgCl$_2$), ATP-regenerating system (1 mM ATP, 0.1 mg/ml creatine kinase, 29 mM creatine phosphate), 10 μM CoA, and 283 nM inhibitor of protease B (IB$_2$). Reactions were incubated at 27°C, and Pho8p activity was assayed in 250 mM Tris-Cl, pH 8.5, 0.4% Triton X-100, 10 mM MgCl$_2$, and 1 mM p-nitrophenyl phosphate. Fusion units were measured by determining the p-nitrophenolate produced as min^{-1} μg^{-1} pep4Δ vacuole, and absorbance was detected at 400 nm.

Tandem affinity purification

Tandem affinity purification (TAP) was performed as described (Puig et al., 2001). Three liters of culture were grown at 30°C to an OD$_{600}$ of ~4, and cells were harvested by centrifugation. Cells were lysed in buffer containing 50 mM 4-(2-hydroxyethyl)-1-piperazineethanesulfonic acid/NaOH, pH 7.4, 300 mM NaCl, 1.5 mM MgCl$_2$, 1× FY protease inhibitor mix (Serva, Heidelberg, Germany), 0.5 mM phenylmethylsulfonyl fluoride, and 1 mM dithiothreitol (DTT). Lysates were centrifuged for 90 min at 100,000 × g, and supernatants were incubated with IgG Sepharose beads for 2 h at 4°C. Beads were isolated by centrifugation at 800 × g for 5 min and washed with 15 ml of lysis buffer containing 0.5 mM DTT. Bound proteins were eluted by tobacco etch virus (TEV) cleavage, and eluates were analyzed on SDS–PAGE. Next the TEV elution buffer was exchanged using NAP-5 columns (GE Healthcare, Piscataway, NJ) equilibrated with vacuole fusion buffer. For HOPS, buffer exchange was omitted, as we could not recover sufficient protein from the column. The TAP buffer inhibits vacuole fusion activity at higher concentrations.

In vitro phosphorylation

TAP-tagged Mon1 was incubated with 500 μl of equilibrated IgG Sepharose bead slurry (4°C, 2 h, nutating). After washing, the beads were equilibrated with fusion reaction buffer and incubated with recombinant Yck3 at 48 μg/ml as a final concentration. Reactions were incubated with ATP-regenerating system or buffer alone for 6 h at 30°C while nutating. Next beads were washed with TEV cleavage buffer. TEV (5 μg/ml) was added to the washed beads and incubated for 2 h at 4°C. Eluted proteins were mixed with 6 ml of calmodulin-binding buffer containing a final concentration of 3 mM CaCl$_2$, mixed with 300 μl of calmodulin Sepharose, and incubated for 1 h at 4°C. The beads where then washed with buffer (20 mM Tris-Cl, pH 7.5, 150 mM NaCl, 1 mM MgCl$_2$, 0.1% Nonidet P-40 alternative, 10% glycerol). Bound protein was eluted with elution buffer containing 5 mM ethylene glycol tetraacetic acid and trichloroacetic acid precipitated. Dried protein was solubilized with SDS buffer and analyzed by immunoblotting.

Preparation of small unilamellar liposomes

The following lipid solutions were prepared: phosphatidylcholine (PC)/phosphatidylethanolamine (PE)/PI3P with lipid concentrations 500/50/50 mM, respectively, and PC/PE with lipid concentrations 500/50 mM, respectively. Lipids were transferred from concentrated stocks to glass test tubes and the solvents evaporated under a nitrogen stream. The test tubes were then run in a SpeedVac for 30 min and stored in a desiccator under vacuum overnight. The next day, the dried lipids were resuspended in MTM1 phosphatase buffer (50 mM sodium acetate, 25 mM Bis-Tris, 25 mM Tris-Cl, pH 6.8, and 5% [wt/vol] glycerol) with vortexing and sonicated in a water bath until the solution was visibly clear.

MTM1 phosphatase assay

A portion of the recombinant His$_6$-MTM1–purified protein was boiled for 10 min and then cooled on ice. Each of the liposome solutions described previously was aliquoted into three 160-μl samples, and 10 μg of MTM-1, boiled MTM-1, or calf intestinal phosphatase was added to individual aliquots. Samples were then incubated and reactions stopped by boiling for 10 min. The lipid and protein components were pelleted by centrifugation and the supernatants decanted. These supernatants were then separated into 50-μl aliquots, and the free phosphatase levels measured by the malachite green phosphatase assay.

Malachite green phosphatase detection

Reactions (50 μl) and blanks were prepared and added to a 96-well plate. Next 10 μl of reagent A (42.8 mM Na$_2$MoO$_4$, 1.14 M HCl) was added to each well, mixed, and incubated at room temperature for 10 min. Then 10 μl of reagent B (0.042% [wt/vol] malachite green, 1% [wt/vol] polyvinyl alcohol) was added to each well, mixed, and incubated for 20 min at room temperature. To stop the reaction, each well received 10 μl of reagent C (7.8% H$_2$SO$_4$), mixed, and incubated for 10 min at room temperature. Free phosphate was measured at 630 nm, and its concentration was derived using a standard curve of P$_i$.

Microscopy

Yeast cells were grown to mid log phase in yeast extract/peptone/dextrose (YPD), yeast extract/peptone/glycerol, or synthetic dextrose complete (SDC) medium lacking selected amino acids or nucleotides, collected by centrifugation, washed once with SDC or synthetic galactose complete (SGC) medium supplemented with all amino acids, and immediately analyzed by fluorescence microscopy. For FM4-64 staining of vacuoles, cells were incubated with 30 μM FM4-64 for 30 min, washed twice with YPD medium, and incubated in the same medium without dye for 1 h. Images were acquired with a Leica DM5500 B microscope equipped with a SPOT Pursuit camera equipped with an internal filter wheel (D460sp, BP460-515, and D580lp; Leica Microsystems, Jena, Germany), fluorescence filters (49002 ET-GFP [fluorescein isothiocyanate/Cy2]: excitation, ET470/40x; emission, ET525/50m; wide green: excitation, D535/50; emission, E590lp; 49008 ET-mCherry, Texas red: excitation, ET560/40x; emission, ET630/75; Chroma Technology, Brattleboro, VT), and MetaMorph 7 software (Visitron Systems, Munich, Germany). Images were processed using ImageJ 1.42 (National Institutes of Health, Bethesda, MD) and AutoQuant X, version 1.3.3 (Media Cybernetics, Bethesda, MD).

REFERENCES

Bishop A, Lane R, Beniston R, Chapa-y-Lazo B, Smythe C, Sudbery P (2010). Hyphal growth in Candida albicans requires the phosphorylation of Sec2 by the Cdc28-Ccn1/Hgc1 kinase. EMBO J 29, 2930–2942.

Boeddinghaus C, Merz AJ, Laage R, Ungermann C (2002). A cycle of Vam7p release from and PtdIns 3-P-dependent rebinding to the yeast vacuole is required for homotypic vacuole fusion. J Cell Biol 157, 79–89.

Brett CL, Plemel RL, Lobingier BT, Vignali M, Fields S, Merz AJ (2008). Efficient termination of vacuolar Rab GTPase signaling requires coordinated action by a GAP and a protein kinase. J Cell Biol 182, 1141–1151.

Brocker C, Kuhlee A, Gatsogiannis C, Balderhaar HJ, Honscher C, Engelbrecht-Vandre S, Ungermann C, Raunser S (2012). Molecular architecture of the multisubunit homotypic fusion and vacuole protein sorting (HOPS) tethering complex. Proc Natl Acad Sci USA 109, 1991–1996.

Cabrera M, Arlt H, Epp N, Lachmann J, Griffith J, Perz A, Reggiori F, Ungermann C (2013). Functional separation of endosomal fusion factors and the CORVET tethering complex in endosome biogenesis. J Biol Chem 288, 5166–5175.

Cabrera M et al. (2010). Phosphorylation of a membrane curvature-sensing motif switches function of the HOPS subunit Vps41 in membrane tethering. J Cell Biol 191, 845–859.

Cabrera M, Nordmann M, Perz A, Schmedt D, Gerondopoulos A, Barr F, Piehler J, Engelbrecht-Vandre S, Ungermann C (2014). The Mon1-Ccz1 GEF activates the Rab7 GTPase Ypt7 via a longin fold-Rab interface and association with PI-3-P-positive membranes. J Cell Sci 127, 1043–1051.

Cabrera M, Ostrowicz CW, Mari M, LaGrassa TJ, Reggiori F, Ungermann C (2009). Vps41 phosphorylation and the Rab Ypt7 control the targeting of the HOPS complex to endosome-vacuole fusion sites. Mol Biol Cell 20, 1937–1948.

Carter SG, Karl DW (1982). Inorganic phosphate assay with malachite green: an improvement and evaluation. J Biochem Biophys Methods 7, 7–13.

Christoforidis S, McBride HM, Burgoyne RD, Zerial M (1999). The Rab5 effector EEA1 is a core component of endosome docking. Nature 397, 621–625.

Degeer J, Boudeau J, Schmidt S, Bedford F, Lamarche-Vane N, Debant A (2013). Tyrosine phosphorylation of the Rho guanine nucleotide exchange factor trio regulates netrin-1/DCC-mediated cortical axon outgrowth. Mol Cell Biol 33, 739–751.

Eitzen G, Will E, Gallwitz D, Haas A, Wickner W (2000). Sequential action of two GTPases to promote vacuole docking and fusion. EMBO J 19, 6713–620.

Esters H, Alexandrov K, Iakovenko A, Ivanova T, Thoma N, Rybin V, Zerial M, Scheidig AJ, Goody RS (2001). Vps9, Rabex-5 and DSS4: proteins with weak but distinct nucleotide-exchange activities for Rab proteins. J Mol Biol 310, 141–156.

Fratti RA, Collins KM, Hickey CM, Wickner W (2007). Stringent 3Q: 1R composition of the SNARE 0-layer can be bypassed for fusion by compensatory SNARE mutation or by lipid bilayer modification. J Biol Chem 282, 14861–14867.

Fratti RA, Jun Y, Merz AJ, Margolis N, Wickner W (2004). Interdependent assembly of specific regulatory lipids and membrane fusion proteins into the vertex ring domain of docked vacuoles. J Cell Biol 167, 1087–1098.

Fratti RA, Wickner W (2007). Distinct targeting and fusion functions of the PX and SNARE domains of yeast vacuolar Vam7p. J Biol Chem 282, 13133–13138.

Gerondopoulos A, Langemeyer L, Liang JR, Linford A, Barr FA (2012). BLOC-3 mutated in Hermansky-Pudlak syndrome is a Rab32/38 guanine nucleotide exchange factor. Curr Biol 22, 2135–2139.

Gillooly DJ, Morrow IC, Lindsay M, Gould R, Bryant NJ, Gaullier JM, Parton RG, Stenmark H (2000). Localization of phosphatidylinositol 3-phosphate in yeast and mammalian cells. EMBO J 19, 4577–488.

Haas A, Conradt B, Wickner W (1994). G-protein ligands inhibit in vitro reactions of vacuole inheritance. J Cell Biol 126, 87–97.

Haas A, Scheglmann D, Lazar T, Gallwitz D, Wickner W (1995). The GTPase Ypt7p of Saccharomyces cerevisiae is required on both partner vacuoles for the homotypic fusion step of vacuole inheritance. EMBO J 14, 5258–5570.

Hama H, Tall GG, Horazdovsky BF (1999). Vps9p is a guanine nucleotide exchange factor involved in vesicle-mediated vacuolar protein transport. J Biol Chem 274, 15284–15291.

Hickey CM, Stroupe C, Wickner W (2009). The major role of the Rab Ypt7p in vacuole fusion is supporting HOPS membrane association. J Biol Chem 284, 16118–16125.

Hickey CM, Wickner W (2010). HOPS initiates vacuole docking by tethering membranes prior to trans-SNARE complex assembly. Mol Biol Cell 21, 2297–2305.

John Peter AT, Lachmann J, Rana M, Bunge M, Cabrera M, Ungermann C (2013). The BLOC-1 complex promotes endosomal maturation by recruiting the Rab5 GTPase-activating protein Msb3. J Cell Biol 201, 97–111.

Jones EW, Zubenko GS, Parker RR (1982). PEP4 gene function is required for expression of several vacuolar hydrolases in Saccharomyces cerevisiae. Genetics 102, 665–677.

Karunakaran S, Sasser T, Rajalekshmi S, Fratti RA (2012). SNAREs, HOPS, and regulatory lipids control the dynamics of vacuolar actin during homotypic fusion. J Cell Sci 14, 650–662.

Kinchen JM, Ravichandran KS (2010). Identification of two evolutionarily conserved genes regulating processing of engulfed apoptotic cells. Nature 464, 778–782.

Kosoff R, Chow HY, Radu M, Chernoff J (2013). Pak2 kinase restrains mast cell Fc{epsilon}RI receptor signaling through modulation of Rho protein guanine nucleotide exchange factor (GEF) activity. J Biol Chem 288, 974–983.

Kucharczyk R, Kierzek AM, Slonimski PP, Rytka J (2001). The Ccz1 protein interacts with Ypt7 GTPase during fusion of multiple transport intermediates with the vacuole in S. cerevisiae. J Cell Sci 114, 3137–3145.

Lachmann J, Barr FA, Ungermann C (2012). The Msb3/Gyp3 GAP controls the activity of the Rab GTPases Vps21 and Ypt7 at endosomes and vacuoles. Mol Biol Cell 23, 2516–2526.

LaGrassa TJ, Ungermann C (2005). The vacuolar kinase Yck3 maintains organelle fragmentation by regulating the HOPS tethering complex. J Cell Biol 168, 401–414.

Longtine MS, McKenzie A3rd, Demarini DJ, Shah NG, Wach A, Brachat A, Philippsen P, Pringle JR (1998). Additional modules for versatile and economical PCR-based gene deletion and modification in Saccharomyces cerevisiae. Yeast 14, 953–961.

Maehama T, Taylor GS, Slama JT, Dixon JE (2000). A sensitive assay for phosphoinositide phosphatases. Anal Biochem 279, 248–250.

Mayer A, Wickner W (1997). Docking of yeast vacuoles is catalyzed by the Ras-like GTPase Ypt7p after symmetric priming by Sec18p (NSF). J Cell Biol 136, 307–317.

Mayer A, Wickner W, Haas A (1996). Sec18p (NSF)-driven release of Sec17p (alpha-SNAP) can precede docking and fusion of yeast vacuoles. Cell 85, 83–94.

McBride HM, Rybin V, Murphy C, Giner A, Teasdale R, Zerial M (1999). Oligomeric complexes link Rab5 effectors with NSF and drive membrane fusion via interactions between EEA1 and syntaxin 13. Cell 98, 377–386.

Merz AJ, Wickner W (2004). Trans-SNARE interactions elicit Ca2 +efflux from the yeast vacuole lumen. J Cell Biol 164, 195–206.

Mizuno-Yamasaki E, Medkova M, Coleman J, Novick P (2010). Phosphatidylinositol 4-phosphate controls both membrane recruitment and a regulatory switch of the Rab GEF Sec2p. Dev Cell 18, 828–840.

Nordmann M, Cabrera M, Perz A, Brocker C, Ostrowicz C, Engelbrecht-Vandre S, Ungermann C (2010). The Mon1-Ccz1 complex is the GEF of the late endosomal Rab7 homolog Ypt7. Curr Biol 20, 1654–1659.

Ostrowicz CW, Brocker C, Ahnert F, Nordmann M, Lachmann J, Peplowska K, Perz A, Auffarth K, Engelbrecht-Vandre S, Ungermann C (2010). Defined subunit arrangement and Rab interactions are required for functionality of the HOPS tethering complex. Traffic 11, 1334–1346.

Peplowska K, Markgraf DF, Ostrowicz CW, Bange G, Ungermann C (2007). The CORVET tethering complex interacts with the yeast Rab5 homolog Vps21 and is involved in endo-lysosomal biogenesis. Dev Cell 12, 739–750.

Poteryaev D, Datta S, Ackema K, Zerial M, Spang A (2010). Identification of the switch in early-to-late endosome transition. Cell 141, 497–508.

Price A, Seals D, Wickner W, Ungermann C (2000). The docking stage of yeast vacuole fusion requires the transfer of proteins from a cis-SNARE complex to a Rab/Ypt protein. J Cell Biol 148, 1231–128.

Puig O, Caspary F, Rigaut G, Rutz B, Bouveret E, Bragado-Nilsson E, Wilm M, Seraphin B (2001). The tandem affinity purification (TAP) method: a general procedure of protein complex purification. Methods 24, 218–229.

Rivera-Molina FE, Novick PJ (2009). A Rab GAP cascade defines the boundary between two Rab GTPases on the secretory pathway. Proc Natl Acad Sci USA 106, 14408–14413.

Rybin V, Ullrich O, Rubino M, Alexandrov K, Simon I, Seabra MC, Goody R, Zerial M (1996). GTPase activity of Rab5 acts as a timer for endocytic membrane fusion. Nature 383, 266–269.

Sasser T, Qiu QS, Karunakaran S, Padolina M, Reyes A, Flood B, Smith S, Gonzales C, Fratti RA (2012). Yeast lipin 1 orthologue pah1p regulates vacuole homeostasis and membrane fusion. J Biol Chem 287, 2221–2236.

Schu PV, Takegawa K, Fry MJ, Stack JH, Waterfield MD, Emr SD (1993). Phosphatidylinositol 3-kinase encoded by yeast VPS34 gene essential for protein sorting. Science 260, 88–91.

Stenmark H, Vitale G, Ullrich O, Zerial M (1995). Rabaptin-5 is a direct effector of the small GTPase Rab5 in endocytic membrane fusion. Cell 83, 423–432.

Stroupe C, Collins KM, Fratti RA, Wickner W (2006). Purification of active HOPS complex reveals its affinities for phosphoinositides and the SNARE Vam7p. EMBO J 25, 1579–1589.

Taylor GS, Maehama T, Dixon JE (2000). Inaugural article: myotubularin, a protein tyrosine phosphatase mutated in myotubular myopathy, dephosphorylates the lipid second messenger, phosphatidylinositol 3-phosphate. Proc Natl Acad Sci USA 97, 8910–8915.

Thorngren N, Collins KM, Fratti RA, Wickner W, Merz AJ (2004). A soluble SNARE drives rapid docking, bypassing ATP and Sec17/18p for vacuole fusion. EMBO J 23, 2765–2776.

Ungermann C, von Mollard GF, Jensen ON, Margolis N, Stevens TH, Wickner W (1999). Three v-SNAREs and two t-SNAREs, present in a pentameric cis-SNARE complex on isolated vacuoles, are essential for homotypic fusion. J Cell Biol 145, 1435–1442.

Wang CW, Stromhaug PE, Kauffman EJ, Weisman LS, Klionsky DJ (2003). Yeast homotypic vacuole fusion requires the Ccz1-Mon1 complex during the tethering/docking stage. J Cell Biol 163, 973–985.

Wang CW, Stromhaug PE, Shima J, Klionsky DJ (2002). The Ccz1-Mon1 protein complex is required for the late step of multiple vacuole delivery pathways. J Biol Chem 277, 47917–47927.

Wurmser AE, Sato TK, Emr SD (2000). New component of the vacuolar class C-Vps complex couples nucleotide exchange on the Ypt7 GTPase to SNARE-dependent docking and fusion. J Cell Biol 151, 551–562.

Yousefian J, Troost T, Grawe F, Sasamura T, Fortini M, Klein T (2013). Dmon1 controls recruitment of Rab7 to maturing endosomes in *Drosophila*. J Cell Sci 126, 1583–1594.

Zhu H, Liang Z, Li G (2009). Rabex-5 is a Rab22 effector and mediates a Rab22-Rab5 signaling cascade in endocytosis. Mol Biol Cell 20, 4720–4729.